21st Australasian Fluid Mechanics Conference
Adelaide, Australia
10-13 December 2018

Rich Premixed Flame in a Spatially Developing *n*-Dodecane Jet in Diesel Engine Conditions

Deepak K. Dalakoti[1], Bruno Savard[1], Armin Wehrfritz[1], Marc S. Day[2], John B. Bell[2], and Evatt R. Hawkes[1,3]

[1] School of Mechanical and Manufacturing Engineering
The University of New South Wales, Sydney, NSW, 2052, Australia

[2]Center for Computational Sciences and Engineering
Lawrence Berkeley National Laboratory, Berkeley, CA, 96551-0969, USA

[3]School of Photovoltaic and Renewable Energy Engineering
The University of New South Wales, Sydney, NSW, 2052, Australia

Abstract

Direct numerical simulation of a spatially developing turbulent *n*-dodecane jet flame in diesel engine conditions was conducted. The thermochemical conditions were matched to the Engine Combustion Network's (ECN) Spray A flame with 15% oxygen in the oxidiser. Previous analysis of the flame structure has revealed the presence of a rich flame in the core of the jet. This rich flame is responsible for the production of soot in diesel engines. Understanding the structure and propagation mechanism of this rich flame, i.e. autoignition (a purely chemical process) vs. deflagration (a coupled process of molecular transport and chemistry), would thus help the design of diesel sprays to reduce soot emissions, one of the main pollutants produced in modern diesel engines. In the present study we characterise this rich flame and its propagation mechanism. Visually, the flame appears as a distributed reaction zone which starts near the flame base and persists well downstream in the core of the jet. The flame is stratified and heat release occurs over a wide range of mixture fractions. Analysis of the flame structure has revealed that both low- and high-temperature chemistry combustion modes are active. A significant amount of formaldehyde is observed in this region. Downstream of the rich flame, large concentrations of acetylene, a soot precursor are observed. Comparison of the flame structure in progress variable space to canonical configurations, such as one-dimensional laminar deflagrations and statistically one-dimensional turbulent rich premixed deflagrations in similar thermodynamic conditions, has revealed that the mean flame structure resembles that of both laminar and turbulent deflagrations. This flame structure is however significantly different from that of zero-dimensional and one-dimensional laminar autoignitions. These observations indicate that deflagration plays a leading role in the propagation mechanism of the present rich flame.

Introduction

To improve the efficiency and reduce the emissions of diesel engines, in-depth understanding of the combustion processes is required. Our understanding of combustion in diesel engine conditions is however limited. This is due to difficulty in performing experiments and extremely high computational cost associated with high fidelity simulations. To focus research efforts of the combustion community, the Engine Combustion Network (ECN) [1] provides a well defined parameter set for detailed investigation of combustion in engine conditions. The ECN Spray A flame [1], which represents combustion in a typical heavy duty diesel engine with moderate exhaust gas recirculation has been a target of several experimental and numerical studies and is considered in this work.

Experimental studies of the Spray A flame [7], which typically measure OH* chemiluminescence and OH/CH_2O planer laser-induced florescence (PLIF) have revealed the global flame structure. A high-temperature chemistry (HTC) nonpremixed flame identified as regions of high OH concentration envelopes the jet. Low-temperature chemistry (LTC), identified as regions of high CH_2O concentration is observed upstream of the start of HTC. A rich HTC flame is observed in the central region of the jet near and downstream of the flame base where LTC products are consumed. Further downstream, soot and its precursors are observed. This flame structure is consistent with the conceptual modes of diesel engine combustion [4, 5].

Numerical investigation of Spray A has been mostly conducted using large-eddy (LES) and Reynolds-averaged Navier–Stokes (RANS) simulation methodologies [9, 8, 6, 14]. These studies have shown that the quasi-steady flame consists of a region of LTC upstream of the flame base, a nonpremixed flame which envelopes the jet, a rich HTC flame in the central region of the jet. Soot is formed in the central region of the jet downstream of the rich HTC flame. This flame structure is consistent with the results of the experimental studies.

Although experimental and numerical studies discussed above have successfully identified the global flame structure, detailed characteristics of the flame are still not available. Of special interest is the premixed flame which occurs in rich mixtures in the core of the jet. This flame is responsible for the formation of soot, one of the main pollutants from the diesel engines. Detailed understanding of this flame will help mitigate the problem of soot. However, not much is know about this flame. Recently, Savard et al. [12] investigated statistically one-dimensional (1D) turbulent rich premixed *n*-dodecane flames in Spray A thermochemical conditions, *i.e.* 60 atm ambient pressure, 21% volume fraction of O_2 in oxidiser at 900 K for equivalence ratios of 3, 5 and 7. The flame presented a distributed low-temperature reaction zone followed by a thin corrugated HTC reaction zone. These observations were largely consistent for all equivalence ratio cases. Interestingly, the turbulent flame structure in progress variable space was found to be well approximated by laminar deflagration while being significantly different than laminar/0D ignitions.

The structure of rich premixed flames is further studied in a follow-up study by Savard et al. [11]. Statistically 1D turbulent rich premixed *n*-dodecane flames at 60 atm ambient pressure and 15% volume fraction of O_2 in oxidiser at 900 K are considered for a range of turbulence intensities and equivalence ratios. The flames are shown to transition from ignition fronts to propagating flames upon increasing the turbulence intensity. Comparison of the turbulent flame structure in progress variable space to laminar flames reveals a transition from a laminar ignition like structure to a laminar deflagration like structure

corresponding to a change in stabilisation mechanism from ignition to propagation upon increasing the turbulence intensity. This change in flame structure is proposed to be a criterion for distinguishing between propagating and igniting flames.

In this study we apply the above criterion to identify the flame characteristic (propagating vs igniting) of the rich premixed flame in a recent direct numerical simulation (DNS) of a spatially developing *n*-dodecane jet flame in Spray A thermochemical conditions. The objectives of this study are:

1. Reveal the structure of the rich HTC flame;
2. Compare the turbulent flame structure in progress variable space to laminar deflagration and homogeneous ignition and thus comment on the stabilisation mechanism of this flame.

The rest of the paper is organised as follows. We first describe the computational methodology followed by the discussion of results and finally conclude the paper.

Methodology

We consider a three-dimensional (3D) computational domain of size $30D \times 30D \times 38D$ in the x, y and z direction, respectively, where z is the axial direction and D (0.17 mm) is the fuel jet diameter. The simulation domain was initialised with quiescent oxidiser at 900 K consisting of 15% O_2 by volume. A fuel jet with a peak mixture fraction of 0.45 at 470 K (a mixture of *n*-dodecane and oxidiser) was impulsively injected into the domain with a bulk velocity of 28 m/s giving a Reynolds number of 17,000 based on the fuel jet properties. Inflow and outflow boundary condition were used at lower and upper z boundaries, respectively. A no-slip wall boundary condition was specified at x and y boundaries. The simulation was conducted for the whole process of two-stage ignition and flame formation. Statistics were collected for the quasi-steady state of the flame.

The DNS was conducted using a low Mach number DNS code called LMC [3]. LMC uses a second order projection method to solve for velocity. A spectral deferred correction (SDC) algorithm is used to solve the species and energy equations. LMC has adaptive mesh refinement capabilities which enable grid refinement in selective regions of the domain. For the present simulation the smallest grid size was 1.25 microns in the regions where LTC occurred, as well as to resolve the edge flame. In the region of the rich premixed flame a 2.5 micron grid was deemed sufficient to resolve the flame based on the flame thickness of 1D rich premixed flame thickness ($\approx$ 30 microns at equivalence ratio of 3). A 53-species 268-reaction *n*-dodecane chemical mechanism [15] was used. For more details of the numerical approach and simulation parameters, see Ref. [2].

For comparison with the turbulent flames, laminar delflagrations and homogeneous ignition (0D ignition) were simulated using FlameMaster [10] for equivalence ratios of 3, 5 and 7. The composition and temperature for these laminar flames were chosen from the adiabatic mixing of liquid *n*-dodecane at 363 K and oxidiser at 900 K, consistent with the DNS.

Results

Figure 1 presents 2D slices (Y-Z plane) of the flame showing heat release rate, mass fraction of $C_{12}H_{25}O_2$ ($Y_{C_{12}H_{25}O_2}$), Y_{CH_2O} and $Y_{C_2H_2}$. The green contour is the iso-line of equivalence ratio of 3 ($\phi = 3$). The blue contour is the iso-line of Y_{OH} at 3.2×10^{-4} (20% of the maximum value in the domain) which bounds the very high temperature zones associated with the nonpremixed flame. A close-up of heat release rate, $Y_{C_{12}H_{25}O_2}$ and Y_{CH_2O} is shown in Fig. 2. In this paper we focus on the rich premixed flame, more specifically the heat releasing region inside the $\phi = 3$ iso-line.

Significant heat release associated with the rich flame can be observed in the core of the jet, near and downstream of the flame base (defined as the start of the nonpremixed flame). The rich flame can be seen burning in both LTC and HTC mode. LTC, identified by $Y_{C_{12}H_{25}O_2}$ (an LTC marker) starts upstream of the nonpremixed flame and persists downstream. CH_2O, an LTC product which is also formed in rich HTC combustion is observed downstream of LTC. Further downstream, large concentration of acetylene (C_2H_2, a soot-precursor) is observed. C_2H_2 is not fully oxidised in the domain and leaves the jet unburned. Other small hydrocarbons are also observed in this region (not shown) which also exit the jet unburned. This flame is thus a source of soot and unburned hydrocarbons in diesel engines. Visually, the flame looks distributed, as can be seen from the heat release contours in Fig. 2. The LTC appears as a broken flame (see $Y_{C_{12}H_{25}O_2}$ contours in Fig. 2) whereas the HTC region is less distributed (see Y_{CH_2O} contours in Fig. 2). This flame structure is visually consistent with moderate to high

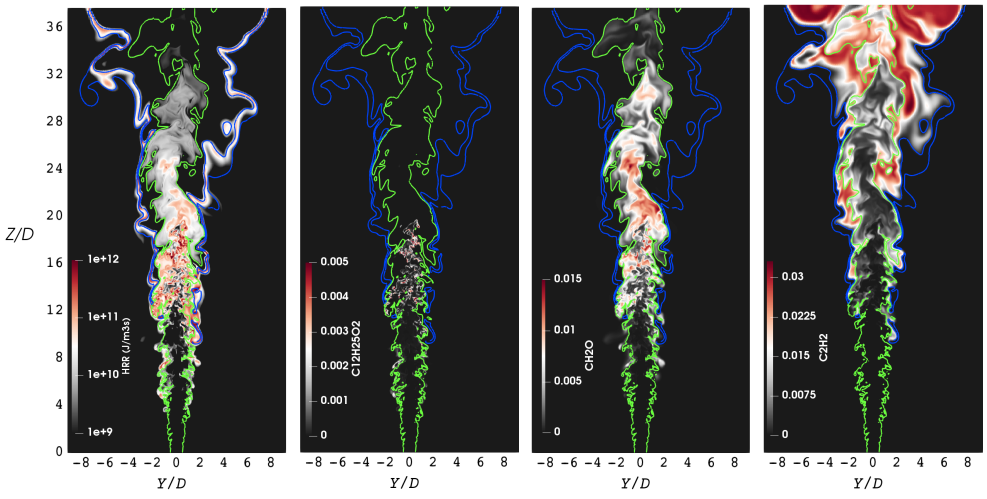

Figure 1: 2D slices (Y-Z plane) of the flame showing heat release rate, $Y_{C_{12}H_{25}O_2}$, Y_{CH_2O} and $Y_{C_2H_2}$. The green contour represents equivalence ratio of 3, the blue contour represents mass fraction of OH at 3.2×10^{-4} (20% of the maximum).

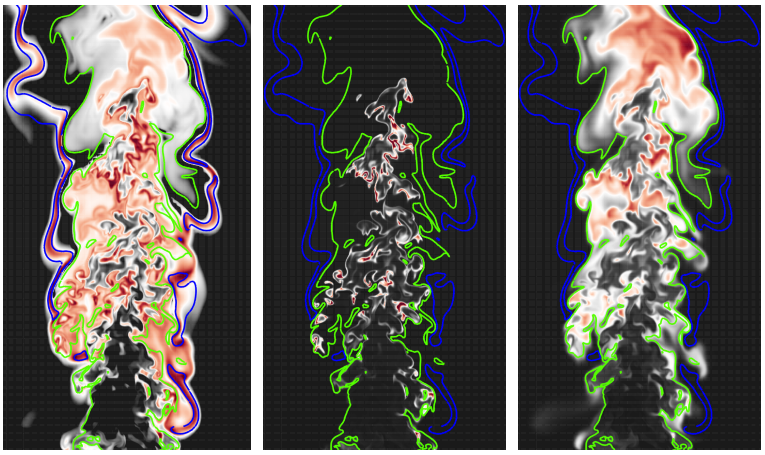

Figure 2: 2D slice (Y-Z plane) of the flame showing a zoomed in view of heat release rate, $Y_{C_{12}H_{25}O_2}$ and Y_{CH_2O}. The figure shows the region between Z/D = 9 and 21. The green contour represents equivalence ratio of 3, the blue contour represents mass fraction of OH at 3.2×10^{-4} (20% of the maximum).

Karlovitz number flames [13, 12] which present thin/broken reaction zones. The flame is axially thick which is typically associated with autoignition fronts, however, previous study of rich premixed flames of *n*-dodecane has shown that this is expected from rich flames at diesel engine conditions [12]. We now study the stabilisation mechanism of this flame. Based on the discussion in introduction, a flame structure (in progress variable space) close to laminar propagating flame is an indicator that the flame has a propagating character while a flame structure close to laminar ignition front indicates towards an ignition character. We use this observation to identify the characteristic of the rich premixed flame, i.e., propagation or ignition in the following.

Figure 3 presents the averaged heat release rate, Y_{CH_2O}, $Y_{C_{12}H_{25}O_2}$ and $Y_{C_2H_2}$ for $\phi = 3$ conditioned on progress variable (c), defined as $c = Y_{H_2O} + Y_{H_2} + Y_{CO} + Y_{CO_2}$. This definition of progress variable is consistent with that used in previous studies [12]. Also presented are corresponding plots from laminar 1D flames with unity Lewis number, laminar 1D flames with mixture averaged transport and 0D ignition. Note that the laminar flames presented here are propagating flames rather than ignition fronts as discussed in the methodology section. A few observations follow, 1) the turbulent flame results are close to the laminar flame results and significantly different from the 0D ignition results and 2) the turbulent flame results are closer to the unity Lewis number laminar flame than the non-unity Lewis number flame which can be attributed to the effects of turbulent mixing which reduces the effects of different molecular diffusivities [13]. Based on the discussion above, the agreement between the turbulent flame results and laminar flames indicates that the flame exhibits a propagating character. Similar analysis is performed for equivalence ratios of 5 and 7, presented in Figs. 4 and 5. Similar to $\phi = 3$ case, the flame structure for $\phi = 5$ and 7 is close to the laminar propagating flame structure with unity Lewis number and significantly different from the 0D ignition case. These observations indicate that the rich premixed flame has a propagating character.

These results indicates that the mean flame structure of turbulent flame with significant mixture stratification and shear can be well predicted by laminar flames. A flamelet based combustion model can thus provide reasonable predictions of the mean flame structure in the conditions of the present flame.

Conclusions

The dataset from a recent direct numerical simulation of a spatially developing *n*-dodecane flame in diesel engine conditions was analysed. The focus of this study was the rich premixed flame present in the core of the jet. The main observations are listed below

1. The flame presents a two-stage combustion structure. The LTC region appears as a broken flame while the HTC regions look like a sheet structure.
2. Large concentrations of C_2H_2 and other small chain hydrocarbons are observed downstream of the flame which exit the domain unburned indicating that this flame is responsible for soot and unburned hydrocarbon emissions.
3. Comparison of the turbulent flame structure in progress variable space to propagating laminar 1D flames (unity Lewis number and mixture-averaged transport) and 0D ignition reveals that the flame structure is well approximated by unity Lewis number laminar flame results and significantly different from the 0D results. This indicates that the turbulent flame has a propagating character. This observation also supports the applicability of flamelet combustion models in the present conditions.

Acknowledgements

This work was supported by the Australian Research Council and computational resources from Pawsey and National Computational Infrastructure awarded through the National Computational Merit Allocation Scheme. The work at LBNL was supported by the Applied Mathematics Program of the DOE Office of Advanced Scientific Computing Research under the U.S. Department of Energy under contract DE-AC02-05CH11231.

References

[1] Engine combustion network. https://ecn.sandia.gov/, accessed 27.06.2018.

[2] Dalakoti, D., Hawkes, E. R., Day, M. S. and Bell, J. B., Direct numerical simulation of two-stage combustion and flame stabilisation in diesel engine-relevant conditions.

[3] Day, M. S. and Bell, J. B., Numerical simulation of laminar reacting flows with complex chemistry, *Combustion Theory and Modelling*, **4**, 2000, 535–556.

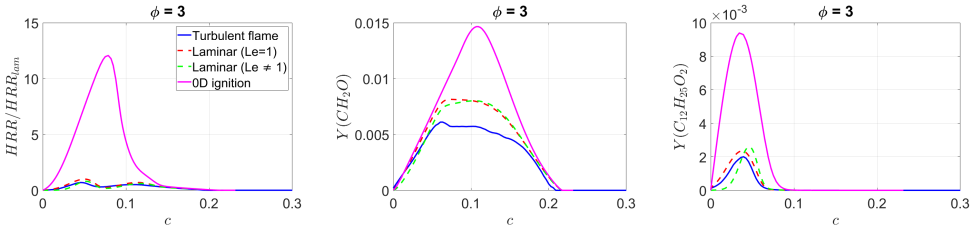

Figure 3: Heat release rate, Y_{CH_2O} and $Y_{C_{12}H_{25}O_2}$ conditioned on progress variable for $\phi = 3$. Note that the heat release rate has been normalised by the maximum value of the unity Lewis number laminar flame.

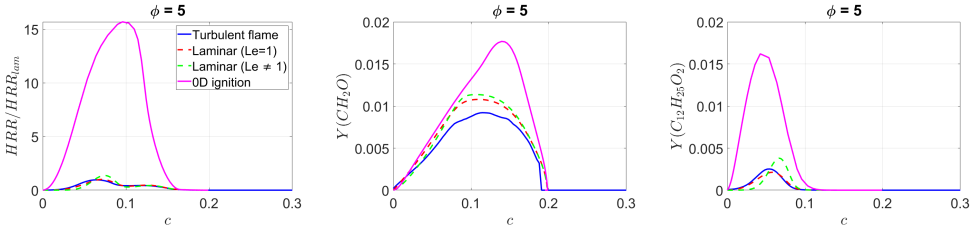

Figure 4: Heat release rate, Y_{CH_2O} and $Y_{C_{12}H_{25}O_2}$ conditioned on progress variable for $\phi = 5$. Note that the heat release rate has been normalised by the maximum value of the unity Lewis number laminar flame.

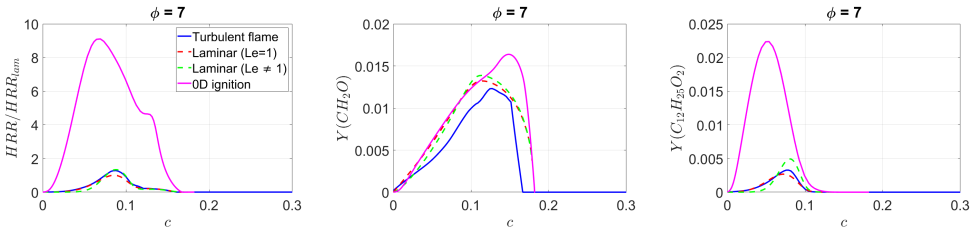

Figure 5: Heat release rate, Y_{CH_2O} and $Y_{C_{12}H_{25}O_2}$ conditioned on progress variable for $\phi = 7$. Note that the heat release rate has been normalised by the maximum value of the unity Lewis number laminar flame.

[4] Dec, J. E., A conceptual model of DI diesel combustion based on laser-sheet imaging, Technical report, SAE Technical paper, 1997.

[5] Idicheria, C. A. and Pickett, L. M., Formaldehyde visualization near lift-off location in a diesel jet, Technical report, SAE Technical Paper, 2006.

[6] Irannejad, A., Banaeizadeh, A. and Jaberi, F., Large eddy simulation of turbulent spray combustion, *Combustion and Flame*, **162**, 2015, 431–450.

[7] Maes, N., Meijer, M., Dam, N., Somers, B., Baya, H., Bruneaux, G., Skeen, S. A., Pickett, L. M. and Manin, J., Characterization of Spray A flame structure for parametric variations in ECN constant-volume vessels using chemiluminescence and laser-induced fluorescence, *Combustion and Flame*, **174**, 2016, 138–151.

[8] Pei, Y., Hawkes, E. R., Bolla, M., Kook, S., Goldin, G. M., Yang, Y., Pope, S. B. and Som, S., An analysis of the structure of an *n*-dodecane spray flame using TPDF modelling, *Combustion and Flame*, **168**, 2016, 420–435.

[9] Pei, Y., Som, S., Pomraning, E., Senecal, P. K., Skeen, S. A., Manin, J. and Pickett, L. M., Large eddy simulation of a reacting spray flame with multiple realizations under compression ignition engine conditions, *Combustion and Flame*, **162**, 2015, 4442–4455.

[10] Pitsch, H., Flamemaster: A C++ computer program for 0d combustion and 1d laminar flame calculations, *Cited in*, 81.

[11] Savard, B., Dalakoti, D., Wehrfritz, A. and Hawkes, E., Structure of (very) rich *n*-dodecane premixed turbulent flames in diesel engine conditions: a criterion to distinguish deflagrations from autoignition fronts, in *Proceedings of the Twenty First Australasian Fluid Mechanics Conference*, Australasian Fluid Mechanics Society, 2018.

[12] Savard, B., Wang, H., Wehrfritz, A. and Hawkes, E. R., Direct numerical simulations of rich premixed turbulent *n*-dodecane/air flames at diesel engine conditions, *Proc. Combust. Inst.*.

[13] Wang, H., Hawkes, E. R., Savard, B. and Chen, J. H., Direct numerical simulation of a high Ka CH4/air stratified premixed jet flame, *Combustion and Flame*, **193**, 2018, 229–245.

[14] Wehrfritz, A., Kaario, O., Vuorinen, V. and Somers, B., Large eddy simulation of *n*-dodecane spray flames using Flamelet Generated Manifolds, *Combustion and Flame*, **167**, 2016, 113–131.

[15] Yao, T., Pei, Y., Zhong, B.-J., Som, S., Lu, T. and Luo, K. H., A compact skeletal mechanism for *n*-dodecane with optimized semi-global low-temperature chemistry for diesel engine simulations, *Fuel*, **191**, 2017, 339–349.